ACS APPLIED MATERIALS & INTERFACES

Letter

www.acsami.org

Chemical Method for Improving Both the Electrical Conductivity and Mechanical Properties of Carbon Nanotube Yarn via Intramolecular Cross-Dehydrogenative Coupling

Yong-Mun Choi,[†,‡] Hungo Choo,[†,§] Hyeonuk Yeo,[†] Nam-Ho You,[†] Dong Su Lee,[†] Bon-Cheol Ku,[†] Hwan Chul Kim,[§] Pill-Hoon Bong,[‡] Youngjin Jeong,[⊥] and Munju Goh*[,†]

[†]Institute of Advanced Composite Materials, Korea Institute of Science and Technology (KIST), Eunha-ri san 101, Bondong-eup, Wanju-gun, Jeolabuk-do 565-905, Korea

[‡]Department of Carbon Fusion Engineering, Jeonju University, 45 Baengma-gil, Wansan-gu, Jeonju, Jeolabuk-do 560-759, Korea

[§]Department of Organic Materials and Fiber Engineering, Chonbuk National University, 567 Baekje-daero, Deakjin-gu, Jeonju 561-756, Korea

[⊥]Department of Organic Materials and Fiber Engineering, Soongsil University, 369 Sangdo-ro, Dongjak-gu, Seoul 156-743, Korea

Supporting Information

ABSTRACT: Chemical post-treatment of the carbon nanotube fiber (CNTF) was carried out via intramolecular cross-dehydrogenative coupling (ICDC) with $FeCl_3$ at room temperature. The Raman intensity ratio of the G band to the D band (I_G/I_D ratio) of CNT fiber increased from 2.3 to 4.6 after ICDC reaction. From the XPS measurements, the $A_{C=C}/A_{C-C}$ ratio of the CNT fiber increased from 3.6 to 4.8. It is of keen interest that both the electrical conductivity and tensile strength of CNT yarn improved to 3.5×10^3 S/cm and 420 MPa, which is 180 and 200% higher than that of neat CNT yarn.

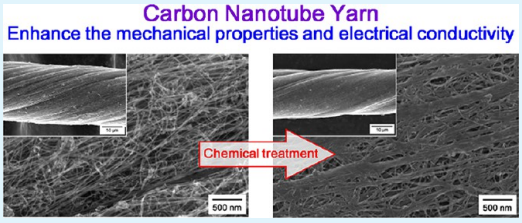

KEYWORDS: *carbon nanotube fiber, $FeCl_3$, intramolecular cross-dehydrogenative coupling*

1. INTRODUCTION

Because carbon nanotubes (CNTs) are cylindrical carbon nanomaterials with a significantly large aspect ratio, they are expected to have excellent mechanical and electrical properties.[1−3] To realize these properties on a macroscopic level, distinctive techniques for integrating the individual CNTs into a large mass are required. Recently, many manufacturing methods for continuous CNT fibers and yarns have been developed. The conventional methods can be classified into four approaches; (i) the coagulation method, which solidifies a CNT-dispersed polymeric material by submerging it in a bath of precipitating liquids;[4] (ii) liquid-crystalline spinning, which bathes the CNT in sulfuric acid and produces liquid crystallinity through wet spinning;[5] (iii) forest spinning, which draws and twists CNTs grown vertically on a substrate;[6] (iv) and the direct spinning method, which uses a vertical CVD furnace.[7] So far, for uniformity and improved mechanical properties, the CNT fiber obtained with the direct spinning method has been shown to be the most effective.[6−8] Indeed, the CNT yarn obtained by this method displayed a tensile strength of 8.8 GPa/SG,[9] which is quite high. Nevertheless, the properties of CNT yarns strongly depend on the synthesizing and manufacturing processes. For this reason, along with the optimization of synthetic methods, chemical post-treatment techniques are utilized to enhance the properties of CNT yarns.

The strategy for producing strong CNT yarn with chemical post-treatment focused on creating a strong chemical bond between individual CNTs. A catecholamine polymer inspired by the mussel[10] along with a polyimide,[11] a photoreactive cross-link,[12−14] chitosan,[15] and aryl diazonium salt[16] successfully enhanced the mechanical properties of CNT yarns. In fact, the tensile strength of CNT yarn fabricated from vertically grown CNTs on substrate was enhanced from 0.55 to 2.5 GPa.[10] Although these experiments led to the improved mechanical properties of CNT yarns, the electrical properties would not be improved because the used organic compounds act as an insulator.

Because graphenes and graphene nanoribbons were successfully synthesized from nonplanar oligophenylene and polyphenylene precursors, cyclodehydrogenation using $FeCl_3$ is currently considered a versatile method to produce planarization and form polycyclic structures via intramolecular cross-dehydrogenative coupling (ICDC).[17−20] Recently, ICDC was adopted to increase the electrical conductivity of reduced graphene oxide by repairing the defect sites.[21] Indeed, electrical conductivity, crystallinity, and the contents of sp^2-hybrized carbon atoms of reduced graphene oxide increased significantly

Received: July 2, 2013
Accepted: August 15, 2013
Published: August 15, 2013

 © 2013 American Chemical Society dx.doi.org/10.1021/am4026104 | ACS Appl. Mater. Interfaces 2013, 5, 7726−7730

after ICDC reaction. The electrical properties were also significantly influenced by the amorphous region of the CNT yarn. Thus, an effective chemical reparation method is essential to improve the electrical conductivity of CNT yarn.

In this study, we will report the ICDC reaction as an effective postchemical treatment for enhancing the electrical conductivity of CNT yarn. This process offers two impressive results: the enhancement of both electrical conductivity and tensile strength.

2. EXPERIMENTAL SECTION

CNT fibers were prepared using the direct spinning method at Soongsil University (Korea).[22] Dichloromethane (≥99.8%), iron(III) chloride ($FeCl_3$; 97%) and nitromethane (≥96%) was provided by Sigma-Aldrich (USA), and methyl alcohol (≥99.5%) by Samchun Chemical Co. (Korea). CNT fibers were added to the dichloromethane (200 mL) and the mixture was then purged with nitrogen gas for 30 min. A solution of $FeCl_3$ in nitromethane (2 mL) was added by drops to the reaction mixture at room temperature in a nitrogen atmosphere over the course of 2 h. The amount of $FeCl_3$ was increased from 0.37 to 3.7 mmol. The flask was sealed and the reaction mixture was stirred at room temperature for 6 to 144 h, and 300 mL of methanol was then added to the mixture and stirred for 5 h to remove residual metal oxides. The product was finally vacuum-dried at 60 °C for 24 h. X-ray photoelectron microscopy (XPS, AXIS-NOVA, Kratos Inc., USA) was applied to discern chemical changes on the surface of the CNT yarn. Al Kα (1485.6 eV) was used as the X-ray source at 14.9 keV of anode voltage, and 4.6 A and 20 mA were applied as the filament current and mission current, respectively. In addition, changes in the intensity ratio between the D-band and G-band with different ICDC reaction time were investigated with Raman spectroscopy. The measurements were taken at room temperature with a 514 nm excitation laser. The electrical conductivity was measured 10 times using the 4-point probe method with the distance (2 cm) between the electrodes (FPP-RS8, Dasol Eng., Korea). CNT yarn was prepared with ca. 20 cm of length and with ca. 18.5 μm of diameter (d). The diameter of CNT yarn was evaluated 30 times using optical microscope (Olympus BX51). Assuming a cylindrical shape, the sample area (A) was calculated as follows, $A = \pi d^2/4$.

3. RESULTS AND DISCUSSION

Raman and X-ray photoelectron spectroscopy (XPS) were performed to examine the changes in chemical bonds of the CNT fiber. The Raman spectra of carbon materials can provide significant information regarding phonon structure, electronic structure, and defect structure. The spectra of highly ordered graphite feature only two Raman-active bands: the in-phase vibration of the graphite lattice (G-band) at 1575 cm^{-1} and the disorder band caused by the graphite edges (D-band) at approximately 1355 cm^{-1}. The G-band originates from in-plane vibrations of sp^2-carbon atoms and is a doubly degenerate phonon mode (E_{2g} symmetry) at the Brillouin zone center. The D-band arises from defects in the carbon structure.[23,24] Therefore, the intensity ratio of the G-band to the D-band (i.e., I_G/I_D) reflects the relative number of sp^2-hybridized carbon atoms on the surface of the CNT fiber. Therefore, changes of the relative number of sp^2-hybridized carbon atoms in the sample can be estimated by determining the I_G/I_D ratio. Figure 1a shows the change in the Raman spectra of CNT fibers with increased ICDC reaction times using 3.7 mmol of $FeCl_3$. The Raman spectra of CNT fibers using 0.37 and 0.74 mmol are shown in Figure S2. The corresponding calculated I_G/I_D ratios of CNT fibers, which treated different concentration of $FeCl_3$, are shown in Figure 1b, increasing significantly with reaction time. Specifically, when 3.7 mmol of $FeCl_3$ was used, the I_G/I_D ratio of CNT fiber was increased from 2.25 to 4.59 after 24 h of ICDC reaction and the I_G/I_D ratio became leveled off and remained constant. However, lower than 3.7 mmol of $FeCl_3$, the I_G/I_D ratio was not reached to level off even after 70 h. Thus, we adapted 3.7 mmol of $FeCl_3$ as an optimal concentration for chemical treatment of CNT fibers.

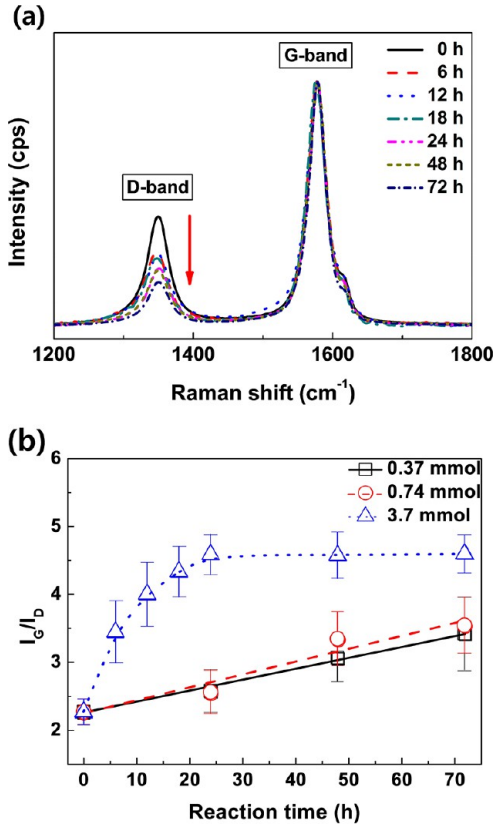

Figure 1. (a) Raman spectra of CNT fiber with different ICDC reaction times using 3.7 mmol of $FeCl_3$, and (b) changes in the I_G/I_D ratio of CNT fibers, which treated different concentrations of $FeCl_3$, as a function of reaction time using.

Panels a and b in Figure 2 show the deconvoluted XPS C1s spectra of neat CNT fiber and CNT fiber after ICDC reaction (CNTF-ICDC) over an 18 h time period, respectively. To identify changes in the surface chemistry, the deconvoluted XPS C1s spectra were fitted to a Gaussian−Lorentzian peak after performing a Shirley background correction. The deconvoluted XPS C1s spectra of neat CNT fiber and CNTF-ICDC (after 18 h of reaction time) showed five characteristics peaks at 284.3, 385.6, 286.7, 287.8, and 288.8 eV. These peaks correspond to sp^2-hybridized carbon,[25] sp^3-hybridized carbon,[25] C−O, C═O, and COO moieties, respectively.[26,27] The measured areas of the peaks corresponding to each chemical bond are listed in Table S2. After ICDC reaction, the intensity of the sp^3-hybridized carbon peak (A_{C-C}) decreased and the peak area of the sp^2-hybridized carbon ($A_{C=C}$) peak increased. Consequently, the $A_{C=C}/A_{C-C}$ ratio of CNTF-ICDC increased from 3.63 to 4.82.

dx.doi.org/10.1021/am4026104 | ACS Appl. Mater. Interfaces 2013, 5, 7726−7730

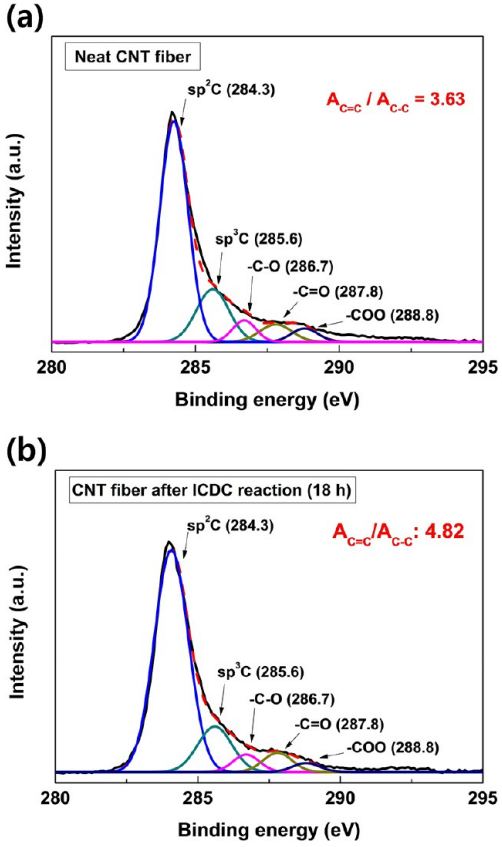

Figure 2. Deconvoluted XPS spectra of the C 1s of (a) neat CNT fiber and (b) CNT fiber after ICDC reaction over 18 h with 3.7 mmol of $FeCl_3$ as a catalyst.

CNT fibers are twisted and fabricated into yarn to evaluate electrical conductivity and mechanical properties. To maintain a consistent width for each strand of yarn, a 3 cm length of CNT fiber was twisted at a constant rate of 240 with a mechanical stirrer. The sample diameters of neat CNT yarn and chemically treated CNT yarn were maintained at approximately ca. 21 ± 3 and 19 ± 4 μm, respectively. The diameter of CNT yarn was measured with a scanning electron microscope (SEM). The SEM images of the neat CNT yarn (Figure 3a, b) and CNT yarn after ICDC reaction (abbreviated as CNTY-ICDC) (Figure 3c, d) are shown in Figure 3. With neat CNT yarn, it was observed that the individual CNT fibers are separated and they display a more twisted length of yarn (Figure 3a, b). In contrast, the CNTY-ICDC displays a closely packed morphology; with individual CNT fibers looking struck together (Figure 3d).

The mechanical properties of CNT fibers with different ICDC reactions were studied, and the typical stress−strain curves are shown in Figure S3. Calculated values, such as tensile strength and modulus, are summarized in Table 1. The CNTY-

Table 1. Mechanical Properties and Electrical Conductivity of Neat CNT Yarn and CNT Yarn after ICDC Reaction with 3.7 mmol of FeCl3 as a Catalyst

sample	ICDC reaction time (h)	tensile strength (MPa)	elongation at failure (%)	electrical conductivity (× 10^3 S/cm)
neat CNT fiber		230 ± 38	7.9 ± 3.0	1.8 ± 0.44
CNT fiber after ICDC reaction	6	260 ± 40	10.1 ± 2.0	2.82 ± 0.42
	12	333 ± 50	11.5 ± 1.6	3.24 ± 0.43
	18	396 ± 55	13.7 ± 1.4	3.35 ± 0.23
	24	420 ± 81	11.1 ± 2.4	3.5 ± 0.21

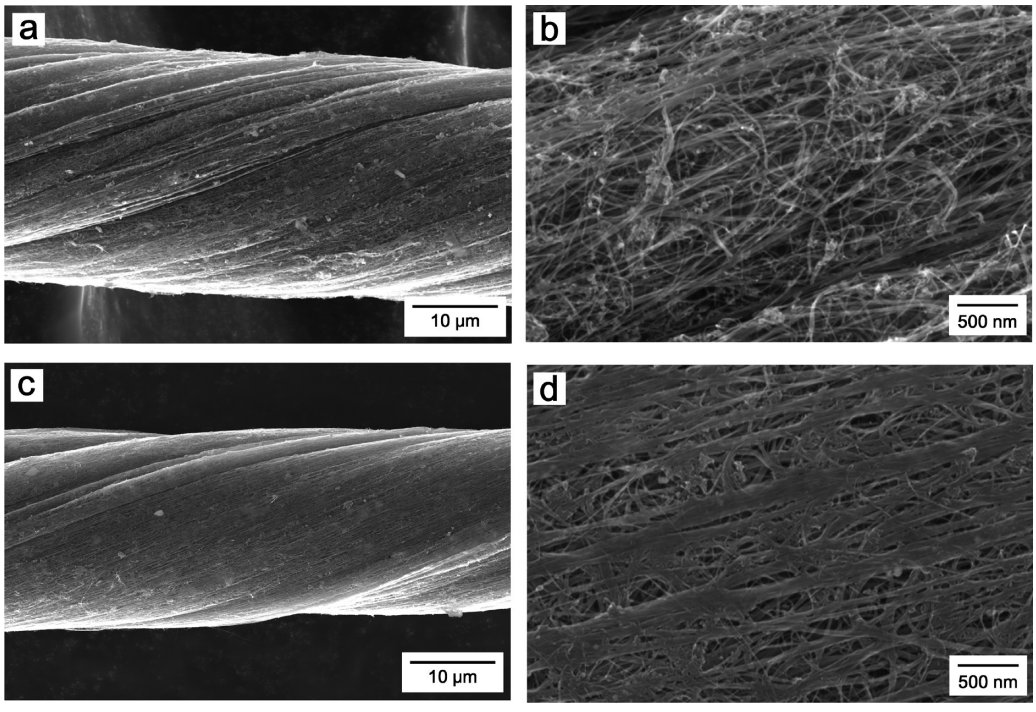

Figure 3. (a, b) SEM images of neat CNT yarn and (c, d) CNT yarn after ICDC reaction over 24 h using 3.7 mmol of $FeCl_3$. The photographs of (b) and (d) show the magnifications of (a) and (c), respectively.

dx.doi.org/10.1021/am4026104 | ACS Appl. Mater. Interfaces 2013, 5, 7726−7730

ICDCs displayed increased tensile modulus and strength compared to neat CNT yarn. In addition, both the tensile strength and modulus of CNT yarns increased as ICDC reaction time increased. In addition, the tensile strength of the CNTY-ICDC over 24 h increased from 230 to 420 MPa, an approximate 180% increase compared to neat CNT yarn (Figure 4a). Such superior mechanical properties can certainly

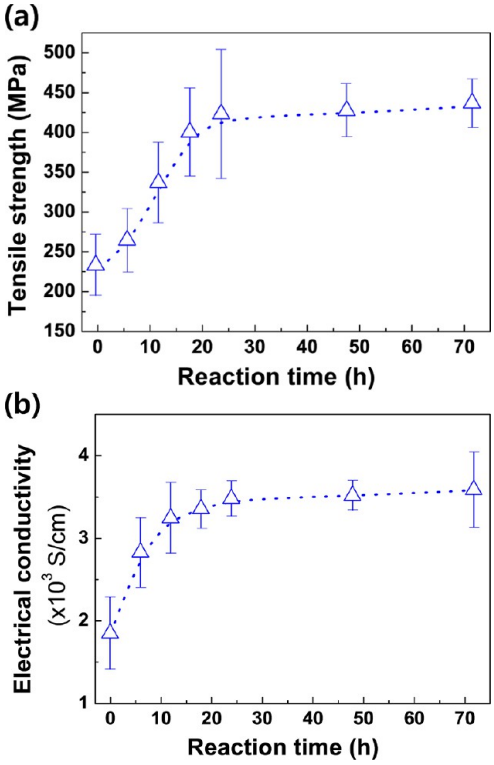

Figure 4. (a) Changes in tensile strength and (b) electrical conductivity of CNT yarns with increasing ICDC reaction times.

be attributed to the increment of crystallinity of CNT fibers (see Figure 1) and the densification effect of CNTY-ICDC (see Figure 3). These factors might be enhancing the interchain interactions between individual CNT fibers.

We also measured the electrical conductivities of CNT yarns before and after ICDC reaction. The electrical conductivities of CNT yarns increased as ICDC reaction time increased (Figure 4b). This can be explained by the restoration of the π-conjugated system of the CNT fiber. That is, the electrical conductivity of CNT yarn is critically dependent on the π-conjugation of the CNT fibers. Through the postchemical treatment process using $FeCl_3$, the defective areas of CNT fibers were successfully restored. As a result, the π-conjugated structure of CNTY-ICDC was expanded beyond that of neat CNT yarn. Eventually, after the ICDC reaction, the electrical conductivity of CNT yarn reached 3.5×10^3 S/cm, which was approximately 200% larger than that of neat CNT yarn (1.8×10^3 S/cm).

It should be mentioned that in many organic and polymeric system, it is notoriously difficult to remove residual metal species from synthesis or doping procedures. Moreover, the residual metal species could cause an enhancement of the electrical conductivity. Thus, the characterization of the residual $FeCl_3$ contents in the chemical-treated CNT fiber and yarns is very essential. We estimated the residual $FeCl_3$ with XPS and Raman spectroscopy. The atomic concentrations listed in Table S3 in the Supporting Information, which were calculated from XPS, show the Fe atom concentration in neat CNT fiber and CNT fiber after ICDC reaction. The Fe atom concentration was decreased from 0.21 to 0.16% after 24 h of ICDC reaction. It is considered that the presence of Fe atom in the neat CNT fiber are comes from the ferrocene catalyst, which are used at a direct spinning method to manufacture the CNT fiber. However, the Fe atom was not increased after the ICDC reaction. Furthermore, we examined the existence of $FeCl_3$ with Raman spectroscopy (see Figure S4 in the Supporting Information). There are no detectable traces of $FeCl_3$ in the CNT fiber after ICDC reaction.

To elucidate the mechanism that leads to the improvements of conductivity and mechanical strength of CNT fiber via ICDC reaction, understanding the type of nanotubes that make up the CNT fiber is important. From TEM observation, we found that the constitutions of CNT fiber are mainly multiwalled CNT (MWNT) and amorphous carbon. We also performed the ICDC reaction of MWNT in order to compare with CNT fiber. The Raman spectroscopy results are shown in Figure S5 in the Supporting Information. Interestingly, the I_G/I_D ratio of MWNT was also increased after ICDC reaction. However, increasing rate is not significant than that of CNT fiber. This means that the increase in the I_G/I_D ratio of CNT fiber is not solely defect healing on MWNT. It is thought that this unexpected large increase on CNT fiber is due to the created carbon networks of amorphous carbon region on the surface of the CNT fiber during the ICDC reaction. By virtue of defect healing on MWNT in CNT fiber and generation of carbon networks of amorphous carbon region, the electrical conductivity could be increased via ICDC reaction. However, healing of defects within the outer layer of the MWNT should have less of an effect on mechanical properties. Thus, it is considered that the cross-link was occurred between interchains of CNT fibers when the creation of carbon networks in amorphous carbon region. Indeed, a closely packed morphology; with individual CNT fibers looking struck together was observed after ICDC reaction (Figure 3). For this reason, the mechanical properties of CNT fiber after ICDC reaction could be increased.

4. CONCLUSION

In this study, an effective method for the postchemical treatment of CNT fibers using ICDC reaction was investigated. We observed a significant increase in the I_G/I_D ratio with increased ICDC reaction times. In addition, the $A_{C=C}/A_{C-C}$ ratio of CNT fibers (after 24 h of reaction time) also increased when compared to that of neat CNT fiber. Furthermore, the electrical conductivity and mechanical properties of CNT yarn were enhanced through ICDC reaction. The method we analyzed in this study proved to be an effective postchemical treatment method of CNT fibers for enhancing both the electrical conductivity and mechanical properties of CNT yarns. So far, the key issue for producing CNT fiber with better mechanical properties is linking the CNTs in the fiber because the CNTs and CNT bundles, without the linker, are bonded only with weak van der Waals interaction. Previous works often used organic materials as the linker and reported the tensile strength enhancement by up to 2 orders of magnitude. However, in this case, the electrical conductivity is normally reduced because the linker acts as an insulating barrier preventing charge tunneling between the CNTs. Our $FeCl_3$

treatment method enhances not only mechanical properties but also electrical conductivity. Although the enhancement of electrical conductivity is only by a factor 2, we believe our work makes an important contribution to the mechanical strength enhancement. Because the $FeCl_3$ treatment does not involve the insulating linkers, we could prevent the degradation in conductivity and after the treatment. Moreover, conductivity was even higher after the treatment. This may be because defects are removed by the treatment and the CNT−CNT interaction is enhanced.

■ ASSOCIATED CONTENT

Supporting Information

Additional data on Raman spectra, XPS, and stress−strain curves. This material is available free of charge via the Internet at http://pubs.acs.org.

■ AUTHOR INFORMATION

Corresponding Author

*E-mail: goh@kist.re.kr.

Notes

The authors declare no competing financial interest.

■ ACKNOWLEDGMENTS

This work was supported by a grant from the Korea Institute of Science and Technology (KIST) Institutional program (2Z03800 and 2Z03870), supported by a grant from the Advanced Technology Center R&D Program funded by the Ministry of Trade, Industry & Energy of Korea (2MR0760), and supported by Nano-Convergence Foundation funded by the Ministry of Science, ICT & Future Planning and the Ministry of Trade, Industry & Energy of Korea (2M32790).

■ REFERENCES

(1) Ruoff, R. S.; Lorents, D. C. *Carbon* **1995**, *33*, 925−930.
(2) Treacy, M. M. J.; Ebbesen, T. W.; Gibson, J. M. *Nature* **1996**, *381*, 678−680.
(3) Tans, S. J.; Devoret, M. H.; Dai, H.; Thess, A.; Smalley, R. E.; Geerlig, L. J.; Dekker, C. *Nature* **1997**, *386*, 474−477.
(4) Vigolo, B.; Penicaud, A.; Coulon, C.; Sauder, C.; Pailler, R.; Journet, C.; Bernier, P.; Poulin, P. *Science* **2000**, *290*, 1331−1334.
(5) Ericson, L. M.; Fan, H.; Peng, H.; Davis, V. A.; Zhou, W.; Sulpizio, J.; Wang, Y.; Booker, R.; Vavro, J.; Guthy, C.; Parra-Vasquez, A. N. G.; Kim, M. J.; Ramesh, S.; Saini, R. K.; Kittrell, C.; Lavin, G.; Schmidt, H.; Adams, W. W.; Billups, W. E.; Pasquali, M.; Hwang, W. −F.; Hauge, R. H.; Fisher, J. E.; Smalley, R. E. *Science* **2004**, *305*, 1447−1450.
(6) Zhang, M.; Atkinson, K. R.; Baughman, R. H. *Science* **2004**, *306*, 1358−1361.
(7) Li, Y.; Kinloch, I. A.; Windle, A. H. *Science* **2004**, *5668*, 276−278.
(8) Shang, Y.; Li, Y.; He, X.; Du, S.; Zhang, L.; Shi, E.; Wu, S.; Li, Z.; Li, P.; Wei, J.; Wang, K.; Zhu, H.; Wu, D.; Cao, A. *ACS Nano* **2013**, *7*, 1446−1453.
(9) Koziol, K.; Vilatela, J.; Moisala, A.; Motta, M.; Cunniff, P.; Sennett, M.; Windle, A. *Science* **2007**, *318*, 1892−1895.
(10) Ryu, S.; Lee, Y.; Hwang, J. W.; Hong, S.; Kim, C.; Park, T. G.; Lee, H.; Hong, S. Y. *Adv. Mater.* **2011**, *23*, 1971−1975.
(11) Fang, C.; Zhao, J.; Jia, J.; Zhang, Z.; Zhang, X.; Li, Q. *Appl. Phys. Lett.* **2010**, *97* (181906), 1−3.
(12) Boncel, S.; Sundaram, R. M.; Windle, A. H.; Koziol, K. K. K. *ACS Nano* **2011**, *5*, 9339−9344.
(13) Min, J.; Cai, J. Y.; Sridhar, M.; Easton, C. D.; Gengenbach, T. R.; Mcdonnell, J.; Humphries, W.; Lucas, S. *Carbon* **2013**, *52*, 520−527.
(14) Filleter, T.; Espinosa, H. D. *Carbon* **2013**, *56*, 1−11.
(15) Ye, Y.; Zhang, X.; Meng, F.; Zhao, J.; Li, Q. *J. Mater. Chem. C* **2013**, *1*, 2009−2013.
(16) Cai, J. Y.; Min, J.; McDonnell, J.; Church, J. S.; Easton, C. D.; Humphries, W.; Lucas, S.; Woodhead, A. L. *Carbon* **2012**, *50*, 4655−4662.
(17) Berresheim, A. J.; Müller, M.; Müllen, K. *Chem. Rev.* **1999**, *99*, 1747−1785.
(18) Zhi, L.; Müllen, K. *J. Mater. Chem.* **2008**, *18*, 1472−1484.
(19) Yang, X.; Dou, X.; Rouhanipour, A.; Zhi, L.; Räder, H. J.; Müllen, K. *J. Am. Chem. Soc.* **2008**, *130*, 4216−4217.
(20) Treier, M.; Pignedoli, C. A.; Laino, T.; Rieger, R.; Müllen, K.; Passerone, D.; Fasel, R. *Nat. Chem.* **2011**, *3*, 61−67.
(21) Park, O. K.; Choi, Y. M.; Hwang, J. Y.; Yang, C. M.; Kim, T. W.; You, N. H.; Koo, H. Y.; Lee, J. H.; Ku, B. C.; Goh, M. *Nanotechnology* **2013**, *24* (185604), 1−7.
(22) Lee, J.; Jung, Y.; Song, J.; Kim, J. S.; Lee, G. −W.; Jeong, H. J.; Jeong, Y. *Carbon* **2012**, *50*, 3889−3896.
(23) Graupner, R. J. *J. Raman Spectrosc.* **2007**, *38*, 673−683.
(24) Ferrari, A. C.; Robertson, J. *J. Phys. Rev. B.* **2000**, *61*, 14095−14107.
(25) Jang, W. S.; Chae, S. S.; Lee, S. J.; Song, K. M.; Baik, H. K. *Carbon* **2012**, *50*, 943−951.
(26) Chen, W.; Yan, L.; Bangal, R. R. *Carbon* **2010**, *48*, 1146−1152.
(27) Pham, V. H. P. H. D.; Dang, T. T.; Hur, S. H.; Kim, E. J.; Kong, B. S.; Kim, S.; Chung, J. S. *J. Mater. Chem.* **2012**, *22*, 10530−10536.